Ministry of Education and Scientific Research
Elmergib University
Faculty of Engineering Al-khoms
Department of Electrical and Computer Engineering
Elmergib Journal of Electrical and Electronic Engineering

وزارة التعليم العالي والبحث العلمي
جامعة المرقب
كلية الهندسة الخمس
قسم الهندسة الكهربائية والحاسوب
مجلة المرقب للهندسة الكهربائية والالكترونية

ISSN: 2959-0450

Volume 2, Issue 3, Dec. 2023

Channel Estimation for Reconfigurable Intelligent Surfaces (RIS) Assisted based on Orthogonal Matching Pursuit (OMP) algorithm

Muamer M. Hawej[1], Haneen M. Khalfallah[2], Takwa M. Belhaj[3]

[1] m.malhwaij@elmergib.edu.ly, Elmergib University, Libya
[2] moftahhaneen56@gmail.com, Elmergib University, Libya
[3] takwamh122@gmail.com, Elmergib University, Libya

Abstract- The tremendous demand for reliable high-speed broadband wireless links is expected to continue growing in the future due to the rapid increase in the number of users, amount of data traffic, and number of applications. The Reconfigurable Intelligent Surfaces (RIS) has been promised as a potential technique for future Sixth-Generation (6G) communication systems. The RIS can passively phase-shift the electromagnetic waves to enhance coverage and capacity at low power and hardware costs. It can provide high beamforming gain that requires accurate channel state information (CSI). The CSI acquisition is too hard to develop for two reasons: First, the passive nature of RIS does not allow the transfer and processing of pilot signals. Second, the dimensions of the cascaded channel between transceivers increase with the large number of RIS elements, which yields high training overhead and computational complexity. In this project, a Time Division Duplex (TDD)-RIS-assisted system is considered, where the CSI in the downlink can be obtained based on the estimated uplink channel. In addition, the cascaded channel i.e. (The cascade of User-RIS and RIS-base station (BS) channels) in RIS-assisted systems shows the sparsity when transformed into the angular domain. Therefore, the channel estimation in the TDD-RIS-assisted system is formulated as a sparse signal recovery problem, which can be solved by Compressed Sensing (CS) algorithms, especially Orthogonal Matching Pursuit (OMP) algorithm and Double Structure-OMP (DS-OMP) approach. The Simulation results demonstrate our proposed OMP approach has significantly improvement compared to the conventional least square estimator. Furthermore, the DS-OMP approach has a small improvement over the OMP algorithm in terms of Normalized Mean Square Error (NMSE) performance. On the other hand, the OMP has less complexity than the DS-OMP.

Keywords: Reconfigurable Intelligent Surfaces (RIS), Time Division Duplex (TDD)-RIS assisted system, Compressed Sensing CS Algorithm, Normalized Mean Square Error (NMSE) performance.

I. INTRODUCTION

Wireless communication systems are changing dramatically as a high data rate and quality of service are in soaring demand. 5G wireless communication has already been released and is currently in service in many countries. Therefore, 6G wireless communication has received the full attention of the researchers. The 6G wireless networks include an ultra-high data rate, high reliability, global coverage, low latency, and high energy efficiency. To meet these requirements, we need more advanced network devices and new techniques for efficient wireless communication. The literature published in recent years suggests that, for 6G, the main ideas are terahertz communication, artificial intelligent and Reconfigurable intelligent surfaces (RISs), also known as intelligent reflecting surfaces (IRSs), or large intelligent surfaces (LISs) [1-6]. The IRS consists of a large number of low-cost passive reflecting elements each being able to reflect the incident signal independently with an adjustable phase shift to collaboratively achieve 3D passive beamforming without the need for any transmit RF chains. It has been proposed to enhance the coverage and capacity of the wireless communication system with low hardware cost and energy consumption [7-10]. In [11], the most important applications of the IRS for the 6G of communication networks are presented. Figure 1 shows when a user is located in a dead zone where the direct link between it and its serving BS is severely blocked

Submitted 01 Nov. 2023; Final Version Received 19 Nov. 2023; Accepted 15 Nov. 2023; Published Online in 09 Dec. 2023

by an obstacle. In this case, deploying an IRS that has clear links with the BS and user helps bypass the obstacle via intelligent signal reflection and thus creates a virtual line-of-sight (LoS) link between them.

Channel Estimation in IRS multi-user communications is a challenging task since it involves the estimation of multiple channels simultaneously. The direct channels between the Base Station (BS) and each user, the channels between the RIS and BS, and the channels between the RIS and each user. This task becomes more complex when the deployed IRSs are equipped with large numbers of unit elements having non-linear hardware characteristics. Furthermore, channel estimation has been widely studied in the conventional wireless communication system [12-15].

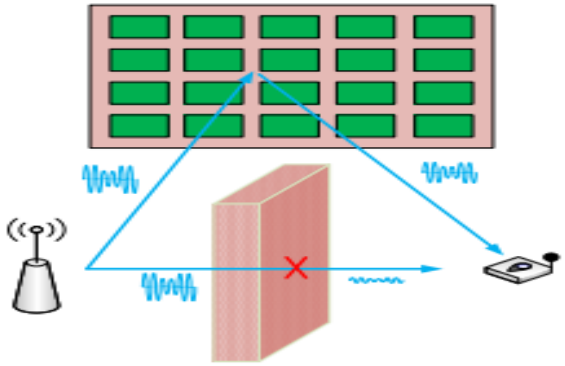

Figure 1. *The user at the dead zone*

There are two main obstacles for conventional schemes to be directly applied in the RIS-assisted system. First, all RIS elements are passive, and cannot transmit, receive, or process any pilot signals to realize channel estimation. Second, since an RIS usually consists of hundreds of elements, the dimension of channels to be estimated is much larger than that in conventional systems, which will result in a sharp increase in the pilot overhead for channel estimation. Therefore, by exploiting the sparsity of the angular cascaded channel (the channel from the user-RIS and the channel from the RIS-BS), the channel estimation problem can be formulated as a sparse signal recovery problem, which can be solved by Compressive sensing (CS) algorithms with reduced pilot overhead [16-19]. The CS algorithms will be illustrated in the next section. The notations used in this paper are as follows.

We use boldface to denote matrices and vectors. $(\boldsymbol{X})^{\mathrm{T}}$, $(\boldsymbol{X})^{*}$ and $(\boldsymbol{X})^{\mathrm{H}}$ stand for the transpose, conjugate, and conjugate transpose of a matrix $\boldsymbol{X}$, respectively. Specifically, $\mathbf{I}_K$ and $\mathbf{I}_M$ denote $K \times K$ and $M \times M$ identity matrices, respectively. $\mathrm{diag}\{\tilde{\sigma}_1(.), \tilde{\sigma}_2(.) \ldots\ldots \tilde{\sigma}_r(.)\}$ denotes a diagonal matrix (.) with $\tilde{\sigma}_1, \tilde{\sigma}_2 \ldots\ldots \tilde{\sigma}_r$ at the main diagonal. $Tr\{.\}$ and $\|.\|_F^2$ are the trace and Frobenius norm of matrix (.), respectively. $\mathcal{CN}(0,\ 1)$ denotes a complex normal distribution with zero mean and unit variance. SVD denotes the singular value decomposition. a $\otimes$ b denotes the Kronecker product of a and b.

This paper was organized as follows: the system and channel models are analyzed in Section **II**. In Section **III,** the compressive sensing logarithms concepts and the channel estimation problem are presented. The computational complexity is discussed in Section **IV.** The simulation results are illustrated and discussed in section **V.** The conclusion is presented in section **VI**.

II. System and Channel Model.

A. Massive MIMO- RIS Assisted System Model

Figure 2 below shows the model of the Massive MIMO-RIS system with one base station (BS) with M-antennas and one RIS assisted with N-elements to serve K single-antenna users [12].

In this paper, an uplink channel estimation in single cell TDD massive multiuser MIMO system with the RIS-assisted system is considered. Due to the channel reciprocity property in the TDD system, the downlink channel can be obtained based on the uplink channel estimation. The received signal $\mathrm{y} \in \mathrm{C}^{\mathrm{M}\times 1}$ at the BS can be expressed by:

$$\boldsymbol{y} = \sum_{k=1}^{K}\left(\boldsymbol{h}_{d,k} + \boldsymbol{G}\,\mathrm{diag}\,(\boldsymbol{\theta})\,\boldsymbol{h}_{r,k}\right)s_k + \boldsymbol{w} \qquad (1)$$

Submitted 01 Nov. 2023; Final Version Received 19 Nov. 2023; Accepted 15 Nov.. 2023; Published Online in 09 Dec. 2023

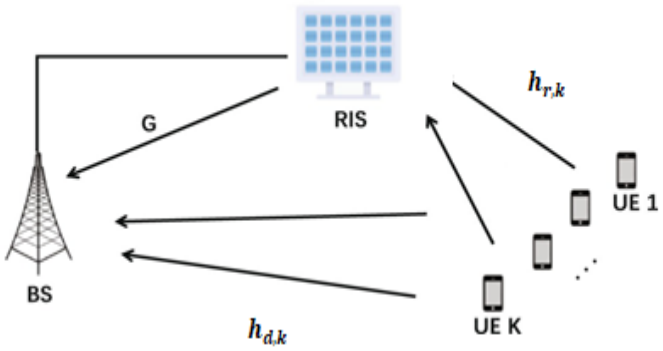

Figure 2. *The RIS-aided uplink multi-user transmission [12]*

where $\mathbf{h}_{d,k} \in \mathbb{C}^{M\times 1}$ is denoted by the direct channel vector between the k^{th} user and the BS, and $\mathbf{G} \in \mathbb{C}^{M\times N}$ is the channel matrix between the RIS and the BS. In (1), $\boldsymbol{h}_{r,k} \in \mathbb{C}^{N\times 1}$ is the received channel vector between the k^{th} user and the RIS. Let s_k is the symbol sent by the k^{th} user, $\boldsymbol{\theta} = [\theta_1, \theta_2, \cdots, \theta_N]^T$ is the reflecting vector at the RIS with θ_n representing the reflecting coefficient for the n RIS element, and $\boldsymbol{w} \in \mathbb{C}^{M\times 1}$ is the received noise vector at the BS. Note that $\theta_n$can be further set as $\theta_n = \beta_n\, e^{j\emptyset n}$, with $\beta_n \in [0, 1]$ and $\emptyset_n \in [0, 2\pi]$ representing the amplitude and the phase for the n_{th} RIS element, respectively. Let $\boldsymbol{H}_k \triangleq \boldsymbol{G}\, diag\,(\boldsymbol{\theta})\, \boldsymbol{h}_{r,k} \in \mathbb{C}^{M\times k}$ represents the cascaded channel between the k^{th} user and the BS via the RIS, and the received signal $\mathbf{y}$ in (1) can be also rewritten as:

$$\boldsymbol{y} = \sum_{k=1}^{K}\left(\boldsymbol{h}_{d,k} + \boldsymbol{H}_k\right)s_k + \boldsymbol{w} \tag{2}$$

In this paper, we assume that the direct channel $\mathbf{h}_{d,k}$ is known for BS, which can be easily estimated as these in conventional wireless communication systems. Therefore, it only focused on the cascaded channel estimation problem which is defined as the channel coefficients from the user to the RIS and the channel from the RIS to the BS.

B. Channel Model:

The channel from the RIS to the BS is denoted by $\mathbf{G} \in C^{M\times N}$, which can be modeled by the widely adopted Saleh-Valenzuela (SV) geometric channel model [14] as follows:

$$\mathbf{G} = \sqrt{\frac{\mathrm{M\times N}}{\mathrm{L_G}}}\ \sum_{l_1}^{L_G} \alpha_{l_1}^{G}\ \boldsymbol{b}\left(\vartheta_{l_1}^{G_r}, \varphi_{l_1}^{G_r}\right)\mathbf{a}\left(\vartheta_{l_1}^{G_t}, \varphi_{l_1}^{G_t}\right)^{\mathbf{T}} \tag{3}$$

where L_G denotes the number of paths between the RIS and the BS. $\mathbf{a}\,(\cdot, \cdot) \in C^{N\times 1}$ and $\mathbf{b}\,(\cdot\ , \cdot) \in C^{M\times 1}$ represent the transmitting and receiving normalized array steering vector associated with the RIS and the BS, respectively. α_{lg}^{G} is the complex gain consisting of path loss, $(\vartheta_{l_1}^{G_r}, \varphi_{l_1}^{G_r})$ is the arrived azimuth (elevation) angle at the BS for the l_1 path. $(\vartheta_{l_1}^{G_t}, \varphi_{l_1}^{G_t})$ is the departed azimuth (elevation) angle at the RIS for the l_1th path. For an $N_1 \times N_2$ Uniform Planer Antenna (UPA), a (ϑ,φ) can be represented by:

$$\mathbf{a}\,(\vartheta, \varphi) = \frac{1}{\sqrt{N}}\left[e^{-\mathrm{j}2\pi d\,\sin(\vartheta)\cos(\varphi)n_1/\lambda}\right]\otimes\left[e^{-\mathrm{j}2\pi d\,\sin(\varphi)n_1/\lambda}\right] \tag{4}$$

where $n_1 = [0, 1, \cdots, N_1 - 1]$ and $n_2 = [0, 1, \cdots, N_2 - 1]$. λ is the carrier wavelength, and d is the antenna spacing usually satisfying $d = \lambda/2$. Similarly, for an $M_1 \times M_2$ UPA (where $M = M_1 \times M_2$), $\mathbf{b}\,(\vartheta, \varphi)$ can be represented by:

$$\mathbf{b}(\vartheta, \varphi) = \frac{1}{\sqrt{N}}\left[e^{-\mathrm{j}2\pi d\sin(\vartheta)\cos(\varphi)m_1/\lambda}\right]\otimes\left[e^{-j2\pi d sin(\vartheta)cos(\varphi)m_2/\lambda}\right] \tag{5}$$

where $m_1 = [0, 1, \cdots, M_1 - 1]$ and $m_2 = [0, 1, \cdots, M_1 - 1]$.On the other hand, the channel $h_{r,k}$ can be represented by :

Submitted 01 Nov. 2023; Final Version Received 19 Nov. 2023; Accepted 15 Nov.. 2023; Published Online in 09 Dec. 2023

$$\mathbf{h}_{\mathrm{r,k}} = \sqrt{\frac{\mathrm{N}}{\mathrm{L}_{\mathrm{r,k}}}} \sum_{l_2=1}^{\mathrm{L}_{\mathrm{r,k}}} \propto_{l_2}^{\mathrm{r,k}} \mathbf{a}(\vartheta_{l_2}^{\mathrm{r,k}}, \varphi_{l_2}^{\mathrm{r,k}}) \tag{6}$$

where $L_{rk}$is the number of paths between the $k^{th}$and the RIS; $\alpha_{l_2}^{r,k}$ represent the complex gain consisting of path loss, $\vartheta_{l_2}^{r,k}(\varphi_{l_2}^{r,k})$ and it then arrived azimuth (elevation) angle at the RIS for the l_2th path. In this paper, we assume all users adopt the well-established orthogonal pilot transmission strategy for the uplink channel estimation and transmit known pilot symbols to the BS via the RIS over T time slots. Specifically, in the t_{th} (t = 1, 2, · · · , T) time slot, the effective received signal $\boldsymbol{y}_{k,t}$ $\in C^{M\times 1}$ at the BS for the k^{th} user after removing the impact of the direct channel can be represented in the time domain as:

$$\boldsymbol{y}_{k,t} = \boldsymbol{G}\ \mathrm{diag}\ (\boldsymbol{\theta}_t)\ \boldsymbol{h}_{r,k} s_{k,t} + \boldsymbol{w}_{k,t} \tag{7}$$

which can be written as

$$\boldsymbol{y}_{k,t} = \boldsymbol{G}\ \mathrm{diag}\ (\boldsymbol{h}_{r,k})\ \boldsymbol{\theta}_t\ s_{k,t} + \boldsymbol{w}_{k,t} \tag{8}$$

where $s_{k,t}$ is the pilot symbol sent by the k_{th} user, $\boldsymbol{\theta}_t = [\theta_{t,1}, \cdots, \theta_{t,N}]^T$ is the $N \times 1$ reflecting vector at the RIS with $\boldsymbol{\theta}_{t,n}$ representing the reflecting coefficient at the n RIS element ($n = 1, \cdots, N$) in the t time slot, $\boldsymbol{w}_{k,t} \sim CN(0, \sigma^2 \mathrm{I}_M)$ is the M × 1 received noise with σ^2representing the noise power. In (8), we denote $\boldsymbol{H}_k = \boldsymbol{G}$ diag $(\boldsymbol{h}_{r,k})$ is the cascaded channel for the k_{th} user. According to the cascaded channel, we can rewrite (8) as:

$$\boldsymbol{y}_{k,t} = \boldsymbol{H}_k\ \boldsymbol{\theta}_t\ s_{k,t} + \boldsymbol{w}_{k,t} \tag{9}$$

After T time slots of pilot transmission, we can obtain the M × T overall measurement matrix $\boldsymbol{Y}_k = [y_{k,1}, \ldots\ldots\ldots\ldots, y_{k,T}]$ by assuming $s_{k,t} = 1$ as

$$\boldsymbol{Y}_k = \boldsymbol{H}_k \boldsymbol{\Theta} + \boldsymbol{W}_k \tag{10}$$

where $\boldsymbol{\Theta} = [\boldsymbol{\theta}_1, \ldots\ldots\ldots\ldots, \boldsymbol{\theta}_T]$ and $\boldsymbol{W}_k = [\boldsymbol{w}_{k,1}, \ldots\ldots\ldots\ldots\ldots, \boldsymbol{w}_{k,T}]$. In (10), the cascaded channel $\mathbf{H}_{\mathrm{k}} \in C^{M\times N}$ in RIS-assisted systems shows the sparsity when transformed into the angular domain. Especially, by using the virtual angular-domain representation, the cascaded channel $\mathbf{H}_{\mathrm{k}}$ can be decomposed as:

$$\mathbf{H}_{\mathrm{k}} = \boldsymbol{U}_M\ \widehat{\boldsymbol{H}}\ \boldsymbol{U}_N^T \tag{11}$$

Here $\widehat{\boldsymbol{H}}$ denotes the M × N angular cascaded channel, $\boldsymbol{U}_{\boldsymbol{M}}$ and $\boldsymbol{U}_N$ are the M × M and N × N dictionary unitary matrices at the BS and the RIS, respectively. By substituting (11) into (10), we can obtain:

$$\boldsymbol{Y}_k = \boldsymbol{U}_M\ \widetilde{\boldsymbol{H}}_k \boldsymbol{U}_N^T\ \boldsymbol{\Theta} + \boldsymbol{W}_k \tag{12}$$

Let denote $\widetilde{\boldsymbol{Y}}_k = (\boldsymbol{U}_M^H \boldsymbol{Y}_K)^H$ as the T × M effective measurement matrix, and $\widetilde{\boldsymbol{W}}_k = (\boldsymbol{U}_M^H \boldsymbol{W}_K)^H$ as the T × M effective noise matrix, (12) can be rewritten as a Compressive sensing (CS) model :

$$\widetilde{\boldsymbol{Y}}_K = \widetilde{\boldsymbol{\Theta}}\ \widetilde{\mathbf{H}}_K^H + \widetilde{\mathbf{W}}_K \tag{13}$$

where $\widetilde{\boldsymbol{\Theta}}_k = (\mathbf{U}_N^T \boldsymbol{\Theta})^H$ is the T× N sensing matrix. Unfortunately, it is difficult to estimate the RIS related to the cascaded channel $\boldsymbol{H}_k$ due to passive RIS elements without signal processing capability. Therefore, Compressive Sensing (CS) is a topic that has recently gained much attention in the applied mathematics and signal processing communities. By exploiting the

Submitted 01 Nov. 2023; Final Version Received 19 Nov. 2023; Accepted 15 Nov.. 2023; Published Online in 09 Dec. 2023
www.ejeee.elmergib.edu.ly Email: ejeee@elmergib.edu.lu Phone No:++218913748971

sparsity of the angular cascaded channel (the sparsity of a signal is defined as the number of non-zero elements in the signal under a certain domain) the channel estimation problem can be formulated as a sparse signal recovery problem, and solved by the CS algorithms [16-19].

III. COMPRESSIVE SENSING (CS) METHOD

The CS technique has been applied in various areas, such as imaging, radar, speech recognition, and data acquisition. In communications, compressive sensing is largely accepted for sparse channel estimation and its variants. With this in mind, compressive sensing promises to estimate the channel with much less pilot overhead or at higher accuracy with a limited number of pilots [16]. The channel estimation of the Massive MIMO System with an assisted System is formulated as a sparse signal recovery problem by exploiting the channel's angular-domain sparsity. In this paper, the popular compressed sensing (CS) algorithms, such as the orthogonal matching pursuit (OMP) techniques are applied to recover the channel at a much reduced number of measurements [20]. Also, the Double Structure-OMP (DS-OMP) based cascaded channel estimation scheme by integrating the double structured sparsity into the classical OMP is discussed and proposed [21].

A. The Proposed Orthogonal Matching Pursuit (OMP) algorithm.

In this section, we explain the compressive sensing method and how it is used in channel estimation. Then, the used algorithm (OMP) is illustrated, also showing the channel model and formulating the cascaded channel estimation problem. The greedy algorithm picks the best immediate choice and never reconsiders its choices. In terms of optimizing a solution, this simply means that the greedy solution will try and find local optimum solutions (which can be many). The most popular algorithms of this type are greedy algorithms, like Matching Pursuit (MP) or Orthogonal Matching Pursuit (OMP), that identify the nonzero elements of x iteratively. A major difference between OMP compared with MP is that OMP will never select the same index twice [20]. The most used greedy algorithm is an orthogonal matching pursuit (OMP) because of its low implementation cost and high speed of recovery. However, when the signal is not very sparse, recovery becomes costly. The idea of OMP is

- An iterative algorithm: it finds x element-by-element in a step-by-step iterative manner.
- A greedy algorithm: at each stage, the problem is solved optimally based on current information.
- From Equation (2), imagine the solution x has only 1 non-zero element, say the 3rd element is non-zero and has the value 0.47 as $\mathbf{x} = [0, 0, 0.47, 0, \ldots, 0]^T$.
- The product Ax will be the 3rd column of **A** multiplied by 0.47. Let a_i denotes the *i*th column of A and x_i denotes the *i*th element of x. The vector $\mathbf{y} = \mathbf{Ax}$ we observed will be $x_3 a_3 = 0.47 a_3$.
- Now, to recover x and given only (**A, y**), a key is to utilize the fact that **x** is sparse.
- In the example, $y = 0.47 a_3$, so y will have the highest correlation towards the 3rd column of **A**.
- We can compute the correlations of b to all the columns of **A**, and see which column gives the "highest correlation". That column tells which index of x is non-zero. This is the "matching" part in OMP.
- The above is the idea behind OMP for 1-sparse x.
- For s-sparse x with s > 1, the same idea applies with one more step: each time a column in **A** is extracted, the effect of the extracted column on vector b has to be "removed" so that next time the same column will not be extracted again. This is the "orthogonal" part of OMP [19].

The description of the OMP would be:

1. Initialize the set of non-zero elements as empty, the observations are set as the residual, $\mathbf{r} = \mathbf{y}$.
2. Correlate all columns of **A** with the residual, $\boldsymbol{A^H}$r, choose the largest element by magnitude and add its index to the set of nonzero elements.
3. With the constraint that only elements of x are nonzero that have been added to the set previously, find an estimate $\hat{x}$ that minimizes$|\boldsymbol{y} - \boldsymbol{A\hat{x}}|^{\mathbf{2}}$.
4. Update the residual as $\mathbf{r} = \mathbf{y} - \mathbf{A\hat{x}}$.

Submitted 01 Nov. 2023; Final Version Received 19 Nov. 2023; Accepted 15 Nov.. 2023; Published Online in 09 Dec. 2023

5. Repeat steps (2 to 4) until either a known s is reached or the norm of the residual $|r|^2$ falls below a predetermined threshold [16].

B. Double-Structured Sparsity of Angular Cascaded Channels

In this section, we propose the DS-OMP-based cascaded channel estimation scheme by integrating the double-structured sparsity into the classical OMP. This algorithm can be summarized in three key stages to detect supports of angular cascaded channels [21]. The description of the three stages would be:

- **Stage 1**: Estimating the completely common row support Ω_r. Since $\{\widetilde{\mathbf{H}}_k\}_{k=1}^{k}$ have the completely common non-zero rows $\{\widetilde{\mathbf{Y}}_k\}_{k=1}^{k}$ can be jointly utilized to estimate the completely common row support Ω_r.
- **Stage 2:** Estimating the partially common column supports $\{\Omega_c^{l1,comm}\}_{l_1=1}^{L}$.
- **Stage 3:** Estimating the individual column supports.

Based on the estimated completely common row support in stage 1 and the estimated partially common column supports in stage 2, it can be estimated the column support $\Omega_c^{l1,k}$ for each non-zero row l_1 and each user k. Through the above three stages, the supports of all angular cascaded channels are estimated by exploiting the double structured sparsity. The angular cascaded channel $\widetilde{\mathbf{H}}_k$ in (10) can be expressed as:

$$\widetilde{\mathbf{H}}_k = \sqrt{\frac{\mathrm{M\,N}}{\mathrm{L_G\,L_{r,k}}}} \sum_{l_1=1}^{L_G} \sum_{l_2=2}^{L_{r,k}} \propto_{l_1}^{G} \propto_{l_2}^{r,k} \tilde{\mathbf{b}}(\vartheta_{l_1}^{G_r}, \varphi_{l_1}^{G_r})\, \tilde{\mathbf{a}}^T(\vartheta_{l_1}^{G_t} + \vartheta_{l_2}^{r,k}, \varphi_{l_1}^{G_t} + \varphi_{l_2}^{r,k}) \tag{14}$$

Based on (14), we can find that each complete reflecting path (l_1, l_2) can provide one non-zero element for $\widetilde{\mathbf{H}}_{\mathrm{k}}$, whose row index depends on $(\vartheta_{l_1}^{G_r}, \varphi_{l_1}^{G_r})$ and column index depends on $(\vartheta_{l_1}^{G_r} + \vartheta_{l_2}^{r,k}, \varphi_{l_1}^{G_t} + \varphi_{l_2}^{r,k})$ Therefore, $\widetilde{\mathbf{H}}_K$ has L_G non-zero rows, where each non-zero row has $L_{r,k}$ non-zero columns. The total number of non-zero elements is $L_G L_{r,k}$ which is usually much smaller than M×N.

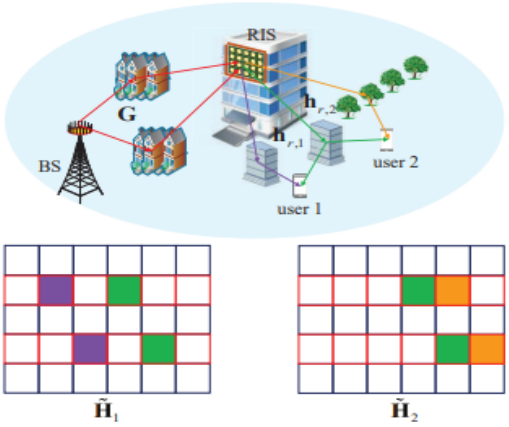

Figure 3. *Double-structured sparsity of the angular cascaded channels [21]*

We can find that different sparse channels $\{\widetilde{\mathbf{H}}_k\}_{k=1}^{K}$ exhibit the double-structured sparsity, as shown in Figure 3. Firstly, since different users communicate with the BS via the common RIS, channel G from the RIS to the BS is common for all users, and the row index is independent of the user index K. The non-zero elements of the angular cascade channel for all users lie on the completely common L_G rows. Secondly, since different users will share part of the scatters between the RIS and users, $\{h_k\}_{k=1}^{K}$ may enjoy partially common paths with the same angles at the RIS. That is to say, for each common non-zero rows

Submitted 01 Nov. 2023; Final Version Received 19 Nov. 2023; Accepted 15 Nov.. 2023; Published Online in 09 Dec. 2023
www.ejeee.elmergib.edu.ly Email: ejeee@elmergib.edu.lu Phone No:++218913748971

l_1 (l_1 =1, 2… L_G), $\{\widetilde{\mathbf{H}}_k\}_{k=1}^{K}$ enjoy L_C common nonzero columns. This is a double-structured sparsity of the angular cascaded channels.

IV. Computational Complexity Analysis

The computational complexity of the DS-OMP algorithm is analyzed in terms of three cases of detecting supports in [21]. First, the computational complexity which calculates the power of M columns of $\tilde{Y}_k$ of size Q × M for k = 1, 2, · · ·, K. The corresponding computational complexity is O (KMQ). Second, for each non-zero row l_1 and each user k, the computational complexity O (N Q $L_{r,k}^3$) is the same as that of the OMP algorithm. Considering L_G K iterations, the overall computational complexity is O (L_G K N Q $L_{r,k}^3$).Finally, the overall computational complexity O (L_GKNQ($L_C - L_{r,k}$)^3). Therefore, the DS-OPM algorithm shows high complexity compared with the OMP algorithm.

V. Simulation Results

In this section, the simulation results for the algorithms methods (the DS-OMP and the OMP) are provided. Initially, we are compared our channel estimation performance in terms of the normalized mean square error (NMSE) with the conventional Least Square estimator and benchmark. Moreover, the effect of important parameters is studied and simulated. For any compressed sensing-based method, the Oracle LS estimator provides us with the best achievable performance. Therefore, the NMSE performance of the OMP and DS-OMP algorithms versus the Oracle least-squares (Oracle-LS) estimator is simulated and compared with the conventional LS estimator to see how results are close to benchmark results. Initially, We set all simulation parameters as the number of the antenna element M = 64, the number of the RIS element N=256, the number of users K=16, the number of paths between the RIS and the BS L_1 =5, the number of paths from the K_{th} user to the RIS L_1 =8, the number of the common paths between the IRS and users L_c =4, and the number of pilots overhead is T.
Figure 4, illustrates the NMSE comparison versus the signal-to-noise ratio (SNR) over practical values ranging from −20 dB to 10 dB. The DS-OMP and the OMP algorithms can achieve better performance in terms of the NMSE compared to the conventional LS method, and we can see the DS-OMP is closer to the Oracle LS estimator than OMP, the difference between these logarithms is very small approximately 2dB. As a result, Despite this simple improvement, The DS-OMP logarithm is more complex than the others, for this reason, a trade-off can be made between the complexities versus the percentage of improvement in terms of NMSE. However, both the CS logarithms method is close to the Oracle LS estimator when SNR is higher. Thus, the best recovery/estimation performance is achieved.

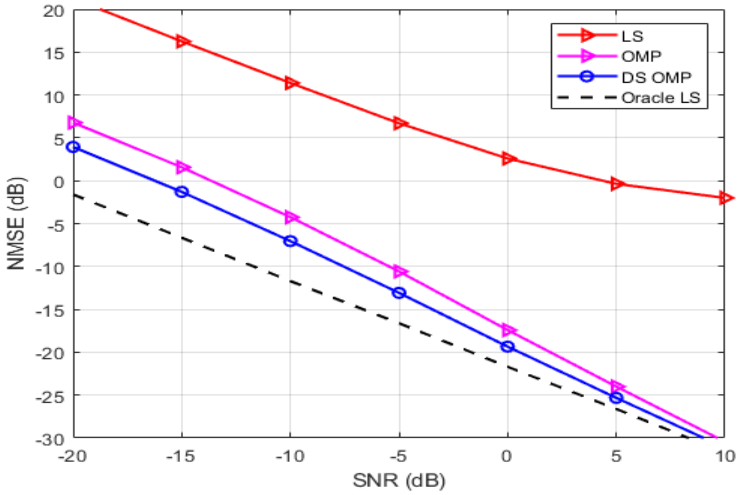

Figure 4. *NMSE performance comparison against the SNR*

Submitted 01 Nov. 2023; Final Version Received 19 Nov. 2023; Accepted 15 Nov.. 2023; Published Online in 09 Dec. 2023
www.ejeee.elmergib.edu.ly Email: ejeee@elmergib.edu.lu Phone No:++218913748971

Figure 5, shows the NMSE versus the pilot overhead T, i.e., the number of time slots T for pilot transmission. The pilot overhead required by the DS-OMP scheme is lower than OMP and both of these are lower than the conventional LS. Note that the NMSE for the LS is high and almost constant when pilot overhead is increased. Furthermore, when T= 32, the NMSE of the OMP is high compared with the DS-OMP, the reason for this, the CSI is not clear enough for the BS to estimate the channel in the time domain (TD) when the pilot is few (T= 32). On the other hand, when the T is greater than 48 the NMSE of the two proposed logarithms and the Oracle LS estimator is very close to each other.

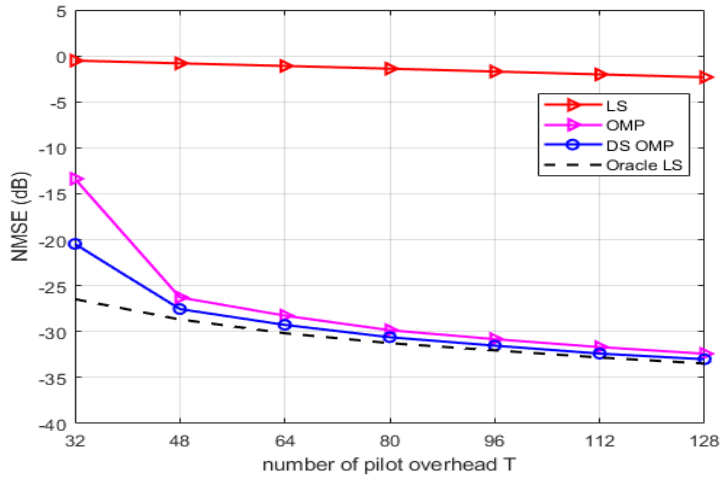

Figure 5. *NMSE performance comparison against the pilot overhead*

Figure 6 shows the CS-based schemes at different values of time slots (T= 32, 48, and 128). It shows the same idea as the previous figure, but in another way to make sure the extent of the difference between both algorithms used in terms of the pilot overhead. Therefore, the proximity in the NMSE value of these logarithms to the same value of T can be observed. Furthermore, when the SNR is greater than 5dB the OMP at T= 32 remains constant compared to the significant decrease in DS-OMP. So, the increase of the SNR doesn't affect the NMSE of the OMP logarithm in the few values of the pilot overhead for the same reason in the previous part. In (T= 48, T= 128), the effect of increasing the SNR is obvious. Based on these previous results, despite this simple improvement of the DS-OMP logarithm, its complexity is high as previously mentioned, for this reason, a trade-off can be made between the complexities versus the percentage of improvement in terms of NMSE. Thus, the study of the effect of the most important parameters on the OMP logarithm method is allocated.

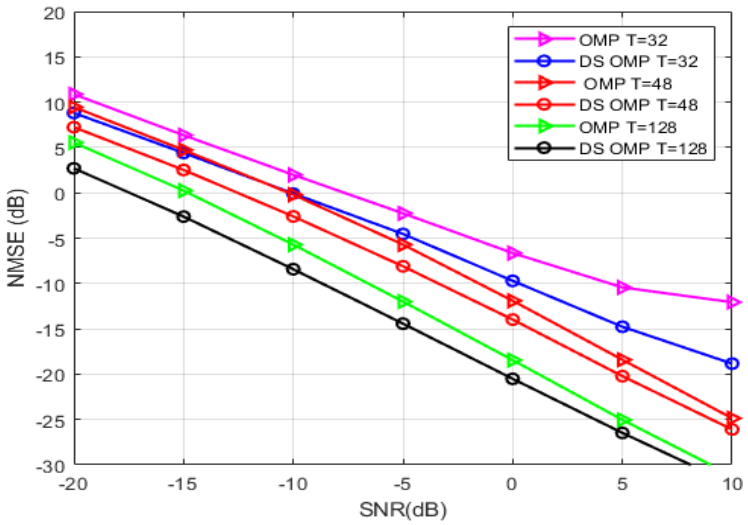

Figure 6. *NMSE performance comparison against the SNR with T∈{32,48,128}*

Submitted 01 Nov. 2023; Final Version Received 19 Nov. 2023; Accepted 15 Nov.. 2023; Published Online in 09 Dec. 2023
www.ejeee.elmergib.edu.ly Email: ejeee@elmergib.edu.lu Phone No:++218913748971

VI. The Effect of Important Parameters of the OMP Algorithm

A. The Antenna Elements (M) Parameter

In this section, the relationship between NMSE and SNR at different values of M (antenna elements) is studied when the other parameters are constant. Also, the effect of the performance in terms of the NMSE versus the number of time slots T is studied at different values of antenna elements M. Figure 7, shows the NMSE versus the SNR at different M ∈{16,64,128}, for both the LS and the CS method, when M increases the NMSE of the CS method decrease at the same value of SNR, but the LS method gives the same NMSE with different values of M, in general, the CS method in a TDD system, the NMSE is inversely proportional to the number of BS antenna M, and LS method independent on the number of M. Therefore, in the RIS assisted communication system with massive antenna gives high performance in the channel estimation.

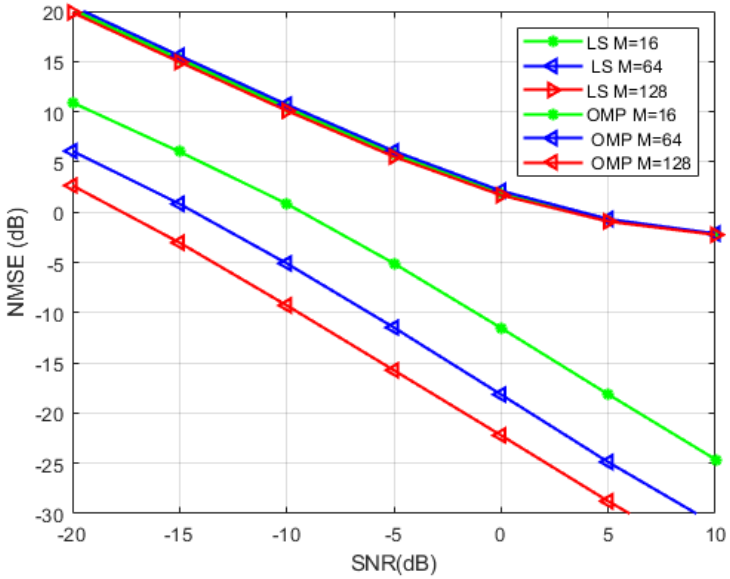

Figure 7. *NMSE performance comparison against the SNR with M∈ {16,64,128}*

Figure 8, shows the repeat of the first experiment, but versus the number of time slots T. At the lowest number of T (T= 32) note that the NMSE for CS method with M∈{64,128} is almost the same and less than M= 16. At T is greater than 32 the difference between the NMSE at M (64,128) is less than 5dB. This can be shown that an increase in the number of BS antenna M, gives a better error performance at a lower number of pilot overhead T, but when T is increased, the effect in M values on the NMSE is not significant. However, the LS method is independent of the number of M and the NMSE remains the same with an increase in T.

Submitted 01 Nov. 2023; Final Version Received 19 Nov. 2023; Accepted 15 Nov.. 2023; Published Online in 09 Dec. 2023
www.ejeee.elmergib.edu.ly Email: ejeee@elmergib.edu.lu Phone No:++218913748971

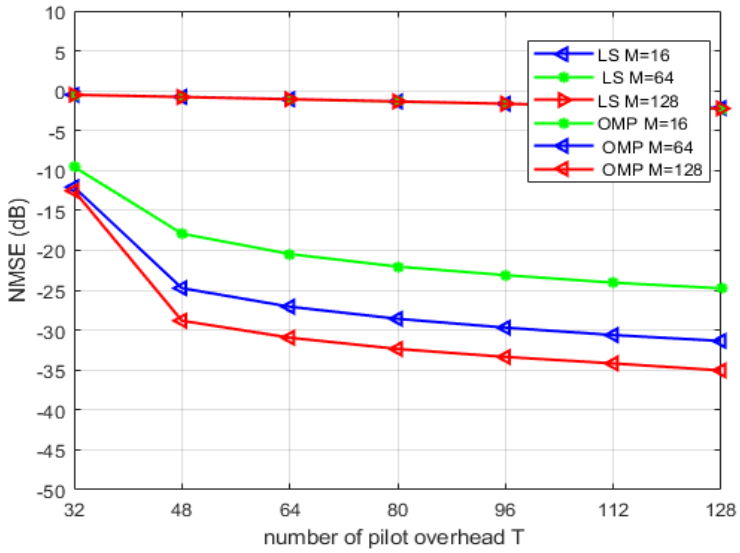

Figure 8. *NMSE performance comparison against the number of the pilot overhead with M∈{16,64,128}*

B. Number of Users (K) Impact

In this section, the number of users K is studied to validate the simulation results. Figure 9, illustrates the NMSE of the CS method for estimating the cascade channel is not affected by the change in the number of user's K, because the number of K affects the size of the cascade channel H matrix but the average of the error remains approximately the same, and in particular, the sparse channel matrices of the cascaded channels of all users have a common sparsity structure due to the common channel between BS and RIS.

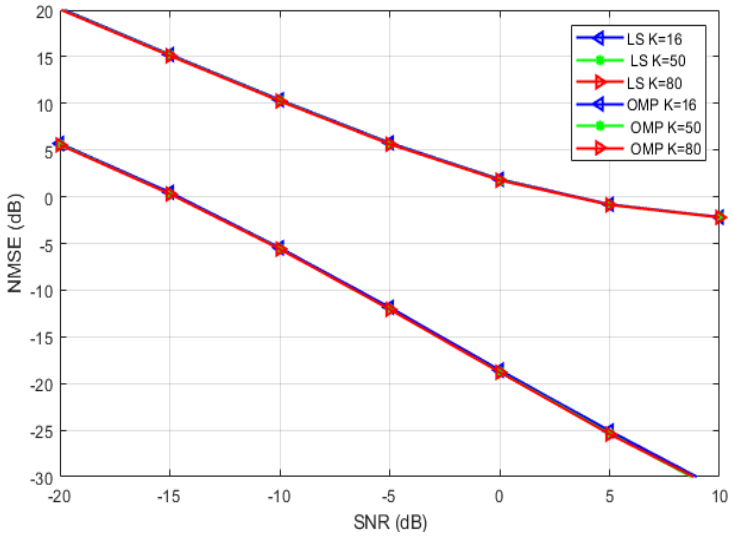

Figure 9. *NMSE performance comparison against the SNR with K∈{16,50,80}*

C. Number of IRS elements (N) Impact

In this section, the number of elements in the IRS N is studied to validate the simulation results. Figure 10 below shows the impact of designing the number of elements in the IRS on the NMSE. The NMSE gaps for all estimators of the OMP method using different value of N is very small (almost the same). But, they show significant improvement in the NMSE performance

Submitted 01 Nov. 2023; Final Version Received 19 Nov. 2023; Accepted 15 Nov.. 2023; Published Online in 09 Dec. 2023
www.ejeee.elmergib.edu.ly Email: ejeee@elmergib.edu.lu Phone No:++218913748971

at N= 64. This illustrates that the proposed method is not affected by the number of elements in IRS because, in a sparse matrix, not all elements are taken into account.

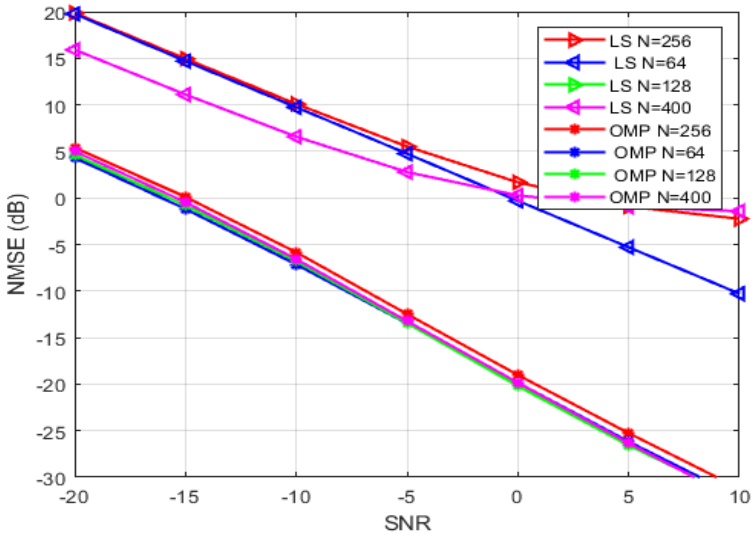

Figure 10. *NMSE performance comparison against the SNR with N∈ {64,128,256,400}*

VII. CONCLUSION

The main concentration of this paper is to study the performance of the 6G uplink channel estimation, which is considered one of the most important challenges. First, the channel estimation solutions are used to reduce the pilot overhead by using compressive sensing algorithms. Then, the main algorithm OMP is simulated and compared with the DS-OMP. The main results can be summarized in the following points: First, the DS- OMP algorithm shows a small improvement in terms of the NMSE with the SNR and the pilot overhead requirement than the OMP algorithm. Furthermore, both algorithms give closer results to the Oracle LS. Second, the conventional LS shows high NMSE and huge pilot overhead requirements. Thus, it can be considered an impractical method in this topic. Third, despite this small improvement of the DS OMP logarithm, its complexity is high in calculation and operation. For this reason, the study of its performance was overlooked, and only the OMP performance was studied (less complexity) with the change in the important parameters with SNR and the pilot overhead requirement. Fourth, a high number of the antenna elements M of the OMP algorithm method gives high performance. Specifically, with high pilot overhead the effect of high M values on the performance is not significant. However, the very high number of antenna elements in M systems has a high cost. Fifth, the sparse channel matrices of the cascaded channels of all users might have a common channel between BS and RIS, this is not considered in the OMP logarithm. Thus the number of user K is not affected in the performance. Finally, the effect of the number of elements in IRS is insignificant because, in a sparse matrix, not all elements are taken into account.

REFERENCES

[1] Y. Liu et al., "Reconfigurable intelligent surfaces: Principles and opportunities," IEEE Communications Surveys & tutorials, vol. 23, no. 3, pp. 1546–1577, May 2021.

[2] E. Basar, M. Di Renzo, J. De Rosny, M. Debbah, M.-S. Alouini, and R. Zhang, "Wireless communications through reconfigurable intelligent surfaces," IEEE Access, vol. 7, pp. 116 753–116 773, August 2019.

[3] D. Perez-Adan, O. Fresnedo, J. P. Gonzalez-Coma, and L. Castedo, "Intelligent reflective surfaces for wireless networks: An overview of applications, approached issues, and open problems," Electronics, vol. 10, no. 19, pp. 2345-2350, September 2021.

[4] Q. Wu, S. Zhang, B. Zheng, C. You, and R. Zhang, "Intelligent reflecting surface-aided wireless communications: A tutorial," IEEE Transactions on Communications, vol. 69, no. 5, pp. 3313–3351, January 2021.

Submitted 01 Nov. 2023; Final Version Received 19 Nov. 2023; Accepted 15 Nov.. 2023; Published Online in 09 Dec. 2023
www.ejeee.elmergib.edu.ly Email: ejeee@elmergib.edu.lu Phone No:++218913748971

[5] S. Nandan and M. A. Rahiman, "Intelligent Reflecting Surface (IRS) assisted mmWave Wireless Communication Systems: A Survey," Journal of Communications, vol. 17, no. 9, September 2022.

[6] Q. Wu and R. Zhang, "Towards Smart and Reconfigurable Environment: Intelligent Reflecting Surface Aided Wireless Network," IEEE Communications Magazine, vol. 58, no. 1, pp. 106 – 112, January 2020.

[7] Q. Wu and R. Zhang, "Intelligent reflecting surface enhanced wireless network via joint active and passive beamforming," IEEE Transactions on Wireless Communications, vol. 18, no. 11, pp. 5394–5409, November 2019.

[8] D. Mishra and H. Johansson, "Channel estimation and low-complexity beamforming design for passive intelligent surface assisted MISO wireless energy transfer," in Proc. IEEE Int. Conf. Acoust., Speech Signal Process. (IEEE ICASSP'19), Brighton, UK, pp. 4659–4663, May 2019.

[9] H.-H. Hsiao, C. H. Chu, and D. P. Tsai, "Fundamentals and Applications of Metasurfaces," Small Methods, vol. 1, no. 4, pp. 1600064, 2017.

[10] Alwazani, Hibatallah, et al. "Intelligent reflecting surface-assisted multi-user MISO communication: Channel estimation and beamforming design." *IEEE Open Journal of the Communications Society*, vol. 1, no.1, pp. 661–680, May 2020.

[11] Wang, Jinghe, et al. "Interplay between RIS and AI in wireless communications: Fundamentals, architectures, applications, and open research problems." *IEEE Journal on Selected Areas in Communications* vol.39, no.8, pp.2271-2288, June 2021.

[12] Wang, Zhaorui, Liang Liu, and Shuguang Cui. "Channel estimation for intelligent reflecting surface assisted multiuser communications." *2020 IEEE Wireless Communications and Networking Conference (WCNC)*. IEEE, 2020.

[13] L. Wei, C. Huang, G. C. Alexandropoulos, C. Yuen, Z. Zhang, and M. Debbah, "Channel Estimation for RIS-Empowered Multi-User MISO Wireless Communications," IEEE Trans. Commun., vol. 69, no. 6, pp. 4144–4157, June 2021.

[14] J. Chen, Y.-C. Liang, H. V. Cheng, and W. Yu, "Channel estimation for reconfigurable intelligent surface aided multi-user MIMO systems," IEEE Transactions on Wireless Communications. Vol. 1, no. 1. Pp. 1-16, February, 2023.

[15] X. Wei, D. Shen, and L. Dai, "Channel estimation for RIS assisted wireless communications: Part I - Fundamentals, Solutions, and Future Opportunities," IEEE Commun. Lett., vol. 25, no. 5, pp. 1403–1407, May 2021.

[16] D.L. Donoho, "Compressed sensing," IEEE Trans. Inf. Theory, vol.52, no.4, pp.1289–1306, April 2006.

[17] C. R. Berger, Z. Wang, J. Huang, and S. Zhou, "Application of compressive sensing to sparse channel estimation," IEEE Commun. Mag., vol. 48, no. 11, pp. 164–174, November. 2010.

[18] K. Hayashi, M. Nagahara, and T. Tanaka, "A User's Guide to Compressed Sensing for Communications Systems," IEICE Trans. Commun., vol. E96.B, no. 3, pp. 685–712, 2013.

[19] S. Qaisar, R. M. Bilal, W. Iqbal, M. Naureen, and S. Lee, "Compressive sensing: From theory to applications, a survey," Journal of Communications and Networks, vol. 15, no. 5, pp. 443–456, October 2013.

[20] Tropp, Joel A., and Anna C. Gilbert. "Signal recovery from random measurements via orthogonal matching pursuit." *IEEE Transactions on Information Theory* vol.53, no.12. pp. 4655-4666, 2007.

[21] X. Wei, D. Shen, and L. Dai, "Channel estimation for RIS assisted wireless communications—Part II: An improved solution based on double-structured sparsity," IEEE Commun. Lett. vol. 25, no. 5, pp. 1403–1407, May 2021.

Submitted 01 Nov. 2023; Final Version Received 19 Nov. 2023; Accepted 15 Nov.. 2023; Published Online in 09 Dec. 2023
www.ejeee.elmergib.edu.ly Email: ejeee@elmergib.edu.lu Phone No:++218913748971